Jour. of the KGS, Vol. 23, No. 9. September 2007, pp. 5～16

Behaviors of Soft Bangkok Clay behind Diaphragm Wall Under Unloading Compression Triaxial Test

삼축압축 하에서 지중연속벽 주변 방콕 연약 점토의 거동

Nghia Trong Le[1] Wanchai Teparaksa[2]

Toshiyuki Mitachi[3] Takayuki Kawaguchi[4]

요 지

비배수 상태에서의 변수 S_u, E_u, n의 함수로 표현되는 단순한 선형 완전점탄성 모델은 굴착 중에 연성 토양에 시공되는 지중연속벽의 변위를 예측하는데 사용된다. 그러나 유한요소해석에서의 이러한 모델은 굴착이 잠시 중단되었거나 완료된 후 지중연속벽의 측방향 변위를 연속적으로 예측하는 데 한계가 있다. 굴착이 이루어지지 않는 동안의 지중연속벽 주변 토양의 변형 거동 특성을 연구하기 위하여, 지중연속벽 주변 토양에 작용하는 응력상태를 가정한 '방콕 연약 점토'에 대한 일련의 삼축압축시험이 모사되었다. 본 연구에서는 세 가지 다른 조건에서의 삼축압축시험이 실시되었는바, 압밀 비배수 조건에서의 재하(CK_oUC), 압밀 배수 및 비배수 조건에서의 재하 및 제하(CK_0DUC와 CK_0UUC)의 조건에서 시험이 실시되었다. 시험으로부터 일련의 CK_0DUC 시험에서 얻은 전단강도는 CK_oUC 시험에서의 잔류강도와 같음을 알 수 있었다. CK_0DUC 시험에서 시험편에 가해지는 수평압력을 점진적으로 감소시키면서 측정한 탄성계수는 편차응력의 증가와 더불어 감소함을 알 수 있었다. 또한 CK_oUC와 CK_0DUC 시험에서 한계상태 관계의 기울기가 동일하게 나타났다. 더욱이, CK_0DUC 시험에서 수평압력을 점진적으로 감소시킬 경우의, 축방향 및 반경방향 변형율 증가율을 시간, 한계상태 관계의 기울기, 편차응력과 평균유효응력의 비의 함수로 표현할 수 있었다. 이 연구는 삼축압축시험의 제하 과정에서 얻은 시험 결과가 굴착 중 지중연속벽의 변형을 예측하는데 사용될 수 있음을 보였다.

Abstract

The simple linear elastic-perfectly plastic model with soil parameters s_u, E_u and n of undrained condition is usually applied to predict the displacement of a constructed diaphragm wall (DW) on soft soils during excavation. However, the application of this soil model for finite element analysis could not interpret the continued increment of the lateral displacement of the DW for the large and deep excavation area both during the elapsed time without activity of excavation and after finishing excavation. To study the characteristic behaviors of soil behind the DW during the periods without excavation, a series of tests on soft Bangkok clay samples are simulated in the same manner as stress condition of soil elements happening behind diaphragm wall by triaxial tests. Three kinds of triaxial tests are carried out in this research: K_0 consolidated undrained compression (CK_0U_C) and K_0 consolidated drained/ undrained unloading compression with periodic decrement of horizontal pressure (CK_0DUC and CK_0UUC). The study shows that the shear strength of series CK_0DUC tests is equal to the residual strength of CK_0UC tests. The Young's modulus determined at each decrement step of the horizontal pressure of soil specimen on CK_0DUC tests decreases with increase in the deviator stress. In addition, the slope of Critical State Line of both CK_0UC and CK_0DUC tests is equal. Moreover, the axial and radial strain rates of each decrement of horizontal pressure step of CK_0DUC tests are established with the function of time, a slope of critical state line and a ratio of deviator and mean effective stress. This study shows that the results of the unloading compression triaxial tests can be used to predict the diaphragm wall deflection during excavation.

Keywords : Diaphragm wall, Elapsed time, Horizontal pressure, Lateral Displacement, Periodic decrement, Triaxial test, Unloading compression

1 Graduate Student, Chulalongkorn Univ., Thailand, nghiacehut@yahoo.com, Corresponding Author
2 Associate Prof. D. Eng., Chulalongkorn Univ., Thailand
3 Prof. D. Eng., Hokkaido Univ., Japan
4 Associate Prof. D. Eng., Hakodate National College of Technology, Japan

1. Introduction

Though a large and deep excavation area takes a long time and many steps to complete, the response of soft clayey soil during and immediately after finishing the excavation is usually considered as undrained condition. The parameters of soil model for back finite element analysis, which is determined from the undrained condition test such as unconfined compression, conventional compression triaxial test, or field-vane-shear test etc., are unchanged in spite of the change of stress condition behind DW during excavation. Moreover, the collected field data of the large and deep excavation show that the displacement of the DW continued increasing both during the elapsed time without activities of excavation and after finishing excavation. Especially, the large area of excavation is divided into many zones and takes a long elapsed time for concreting the basement floors or installing the strut systems. During this elapsed time, the total stress condition of the soil behind the wall is almost unchanged; however, the observed lateral displacement of the retaining wall is non-stopping. Therefore, the creep displacement appears not only on the ground settlement of an embankment but also on the lateral displacement of the retaining wall.

A movement of DW was monitored at the Bank of Thailand (BOT) project, located on the Chao Praya River bank, Bangkok. The project consisted of five underground basement floors with the total depth of excavation about 15.2 m. This project took more than one year to finish all the excavation and top-down construction for the basement floors. The area of excavation was larger than 10,790 m^2, and was divided into thirteen constructed zones. The sequence of basement construction at each zone was shown in Figure 1 and Table 1. The excavation was paused at three main excavated stages 2, 4 and 6 at the depth of 1.25 m, 8.1 m and 15.2 m, respectively. At those stages, there were the elapsed times of excavation to concrete the basement floors before continuing ex-

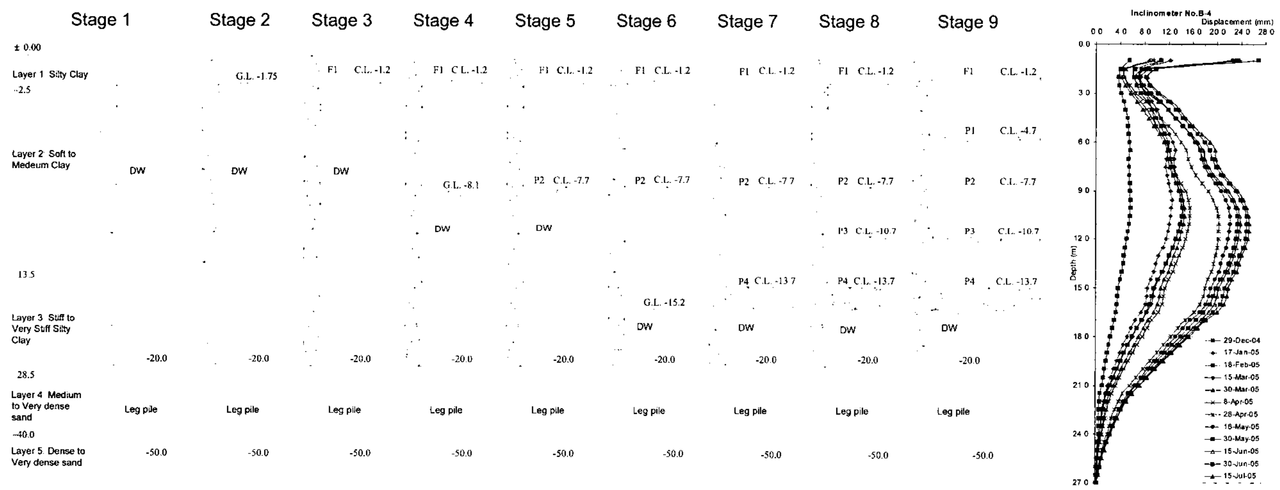

Fig. 1. Process of excavation of top-down construction and inclinometer data of the BOT project

Table 1. The sequence of basement construction of a BOT case history

Stage (1)	Duration (day) (2)	Construction activities (3)
1	1 − 234	Construct diaphragm wall, stanchion and bored pile
2	251 − 313	Excavate to elevation of −1.75 m.
3	330 − 387	Cast floor slab (F1) at elevation of −1.2 m
4	381 − 487	Excavate to elevation of −8.1 m
5	412 − 502	Cast floor slab (P2) at elevation of −7.7 m
6	495 − 642	Excavate to elevation of −15.2 m
7	538 − 662	Cast floor slab (P4) at elevation of −13.7 m
8	517 − 706	Cast floor slab (P3) at elevation of −10.7 m
9	591 − 737	Cast floor slab (P1) at elevation of −4.7 m

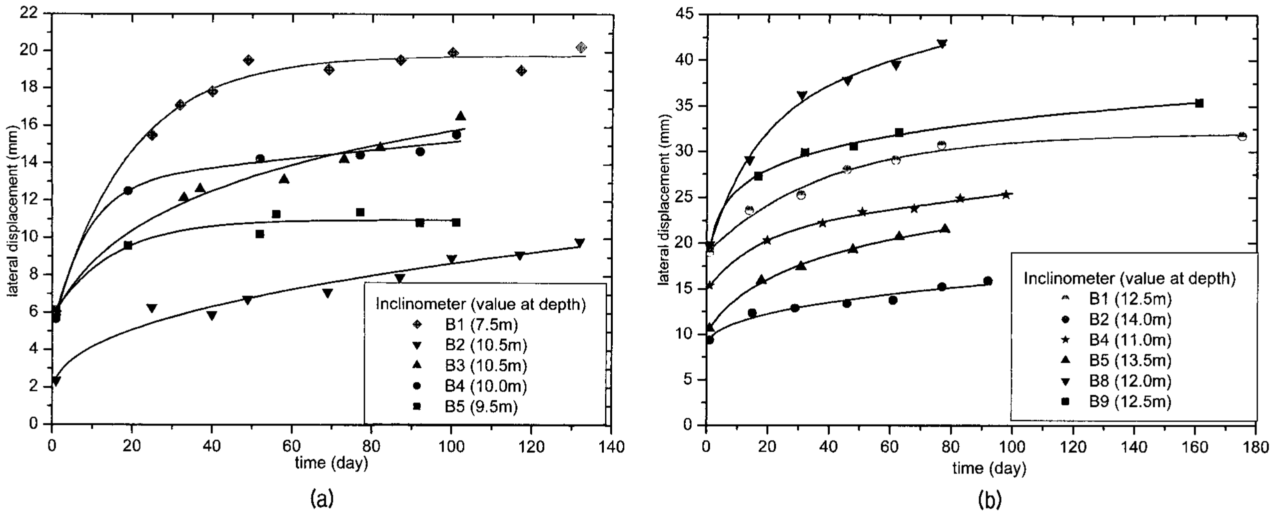

Fig. 2. Lateral displacement of diaphragm wall on the elapsed time excavated to (a) 8.1 m and (b) 15.2 m.

cavation deeper, and the displacement of the DW was continuously increasing.

The lateral displacement of DW was monitored by nine inclinometers installed around the periphery of the DW. Figure 2 showed the data of the DW lateral displacement of some inclinometers (B1 to B9) when the ground level was excavated to 8.1 m and 15.2 m deep. As the excavation paused at 8.1 m deep to cast the floor slab F1, the largest value of lateral displacement appeared at around 2.0 m deeper than the excavated level. It was taken nearly 3 months to cast the F1 floor, and during this period, the inclinometer data monitored biweekly showed a non-stop increase. Figure 2 (b) shows data of the DW lateral displacement when the excavation went through the stiff clayey layer to 15.2 m deep. Especially, the maximum of the DW lateral displacement, which occurred at the depth around 12.5 m of soft clay layer, still increased after 6 months even though the excavation was over at inclinometers B1 and B9.

Many researchers have studied creep behaviors of the natural soil [4]; however, the creep behaviors under unloading compression triaxial test with the periodic decrement of cell pressure have not been considered up to this time. The main purpose of this paper was to observe the behaviors of soil elements behind the DW under the conditions of the undrained and drained unloading compression using triaxial tests. The series of K_0 consolidated unloading compression triaxial tests with undrained and drained conditions (CK_0DUC and CK_0UUC) were carried out to observe the creep deformation of the soil sample. The soil sample simulated the pressure conditions, which were the same as the stress states of the soil elements behind the DW during excavation, to determine its deformation characteristics of both axial and lateral directions versus time. Beside that, the K_0 consolidated undrained compression test (CK_0UC) was also carried out. From the results of CK_0UC tests, the ratio of undrained shear strength and Young's modulus at 0.01% of axial strain ($s_u/E_{u(0.01\%)}$) was calculated and compared with that ratio from back finite element analysis of the other authors. Moreover, the shear strength and slope of critical state line were determined and compared with those obtained from three kinds of triaxial tests CK_0UC, CK_0DUC and CK_0UUC.

2. Material and Testing Procedure

The undisturbed soil samples, with the height of 150 mm and diameter of 75 mm, were taken from two 25.0 m deep boreholes of BOT project near the bank of Chao Praya River in Bangkok. The geotechnical properties of those samples -such as their natural unit weight, water content, Atterberg limits, shear strength and Young's modulus- were presented in Figure 3. Soil specimens of 100 mm height and 50 mm in diameter, were trimmed from those undisturbed samples and then saturated under

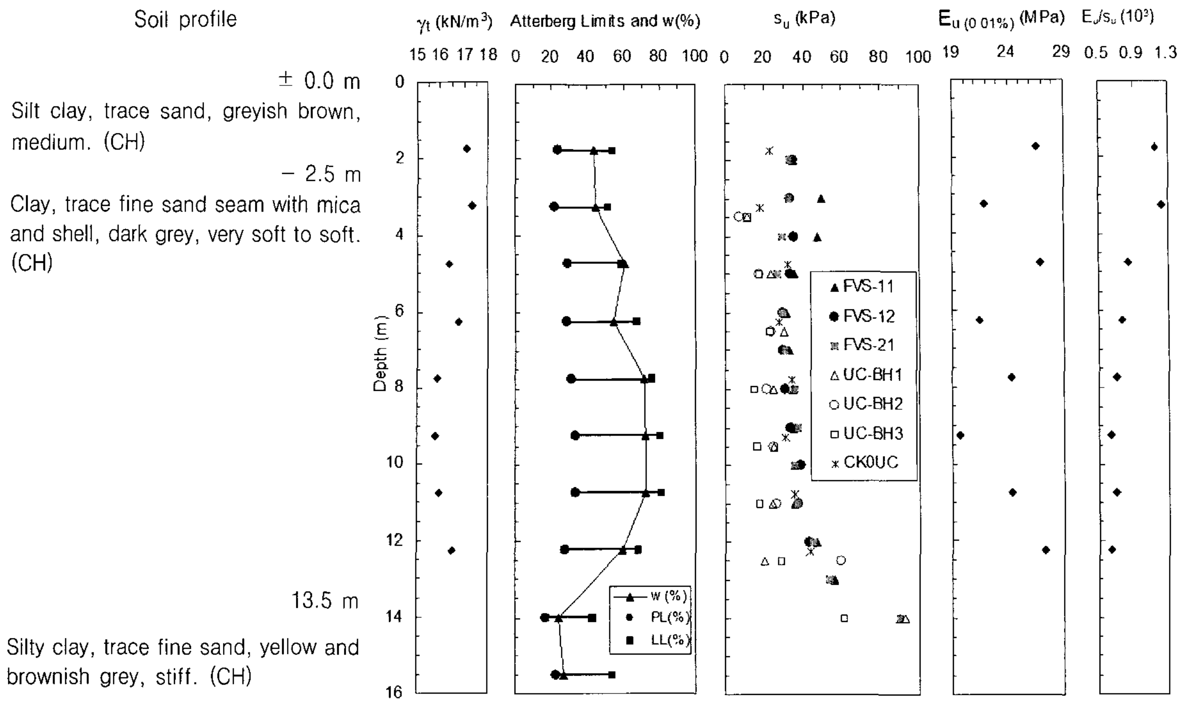

Fig. 3. Geotechnical properties at BOT site

15 kPa of cell pressure and 5 kPa of back pressure at the beginning and gradually increased to final stage at 200 kPa of back pressure and 210 kPa of cell pressure. Those values of pressures dissolved sufficient air on the specimens. The excess of pore water pressure was measured by means of B-value to check the saturation degree of the specimens. Then, all the specimens were consolidated automatically to obtain K_0 condition with the vertical effective stress equal to estimated overburden effective stress at the depth of each sample. The vertical effective stress was gradually increased in 0.5 kPa/min while the cell pressure was automatically controlled to keep the radial strain of the specimen equal to zero. Time duration to stop the K_0 process was after the completion of primary consolidation based on the 3t method of Standard of Japanese Geotechnical Society for Laboratory Shear Test [7]. Eight filter paper strips were put around the side of a soil specimen to enhance the radial drainage during consolidation. Subsequently, we continued carrying out the following tests for the specimens:

(1) CK_0UC (K_0 Consolidated Undrained Compression test): the specimens were sheared under undrained condition as conventional triaxial compression test at 0.1%/min of axial strain rate. The parameters such as applied pressures, deformation and pore water pressure of soil specimen were controlled and recorded automatically by the system of transducers and computer; therefore, the relationship between deviator stress and axial strain was measured nearly 100 steps until the axial strain reached 0.01%. The undrained shear strength (s_u) and undrained Young's modulus at 0.01 % of axial strain ($E_{u(0.01\%)}$) of the samples were determined and shown in Figure 3.

(2) CK_0DUC (Anisotropically Consolidated Drained Unloading Compression test): after anisotropic consolidation to be K_0 condition, the soil specimens were swelled (unloading compression) by periodically decreasing horizontal stress step-by-step while the axial effective stress was maintained constantly. The amplitude of the decrement step of horizontal stress was controlled by the decrement step of stress ratio (DK) from the initial value of effective stress ratio ($K_0 = \sigma'_{h0}/\sigma'_{v0}$) to that value at failure ($K_f = \sigma'_{hf}/\sigma'_{vf}$) as shown in Figure 4. Each reduced value of horizontal stress was kept for 24 hours or 48 hours in some steps. During that time, the cell pressure and axial load were controlled automatically to maintain the vertical and horizontal effective stresses to be

Table 2. Summary of triaxial test results of marine Bangkok clay

Test No.	Depth (m)	Test Condition	ω (%)	e_0	$q_{max}/2\sigma'_{vo}$	ϕ'_r (^{0})	ϕ'_p (^{0})	M	B-value (%)
1	2.0	CK_0UC	43.6	1.30	0.818	46.3	52.8	2.17	97.8
2	3.5		40.6	1.14	0.612	39.5	42.4	1.74	100.1
3	5.0		62.2	1.68	0.642	43.3	52.3	2.15	99.2
4	8.0		81.6	2.26	0.413	35.3	36.7	1.49	99.7
5	9.5		72.9	2.01	0.412	36.9	37.9	1.54	97.1
6	11.0		64.4	1.76	0.440	34.9	38.1	1.55	91.4
7	12.5		59.9	1.67	0.456	34.0	38.1	1.53	98.1
8	5.0	CK_0DUC ($\Delta=-0.05$)	55.4	1.56	0.453	-	62.8	2.53	99.1
9	6.5		55.7	1.54	0.419	-	33.4	1.35	99.8
10	8.0		64.2	1.79	0.374	-	39.7	1.61	97.1
11	9.5		64.8	1.78	0.368	-	38.7	1.55	92.1
12	11.0		71.8	2.00	0.360	-	36.9	1.50	100.1
13	10.5	CK_0DUC ($\Delta=-0.10$)	74.3	2.06	0.344	-	33.4	1.35	100.3
14	12.0		64.4	1.82	0.381	-	38.7	1.58	98.3
15	6.0	CK_0UUC ($\Delta=-0.05$)	71.3	2.04	0.443	-	38.7	1.58	96.7
16	9.5		77.7	2.12	0.351	-	40.6	1.66	97.3
17	11.0		76.1	2.12	0.505	-	33.4	1.35	97.0

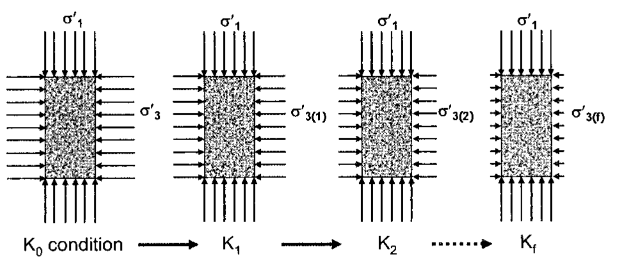

Fig. 4. Procedure of CK_0DUC and CK_0UUC tests

unchanged. The valve of back pressure was opened for drained condition, and the back pressure was supplied continuously with the value 200 kPa as the final value of K_0 consolidation stage. The volume strain of the sample was determined from the volume of water in the burette by a differential pressure transducer.

(3) CK_0UUC (Anisotropically Consolidated Undrained Unloading Compression test): this test was the same as the test number (2); however, the drainage valve was closed for undrained condition.

In other words, the soil specimens were applied periodically to the increment of deviator stress until reaching rupture in CK_0DUC and CK_0UUC tests. We only considered the effect of soil behaviors on displacement of DW during excavation; therefore, for tests (2) and (3), the maintenance time for each loading step was only 24 hours or 48 hours for some steps. To eliminate the influence of temperature as a variable, the temperature during the experiments was kept as constant to be 24 ± 1^0C. We carried out three kinds of tests seventeen soil samples for and these test results were summarized in Table 2.

3. Test Results and Discussions

3.1 Shear Strength and Young's Modulus

The undrained shear strength (s_u) of three kinds of tests -such as field vane shear test, unconfined compression and CK_0UC tests- versus depth was shown in the Figure 3. Based on the Figure 3 and Table 2, the ratio of undrained shear strength and overburden effective stress (s_u/σ'_{v0}) of CK_0UC tests was approximated to that ratio of field vane shear (FVS) test. The overburden effective stress (σ'_{v0}) was estimated from the natural unit weight of the tested soil samples and 2.0 m depth of ground water level. Upper 5.0 m depth, the ratio s_u/σ'_{v0} was larger than 0.5 because of the effect of weathered consolidation to this clay layer. This ratio was around 0.45 for the depth from 5.0 m to 13.0 m. This finding was similar to the result of the test at 11.0 m depth in Sutthisan area by

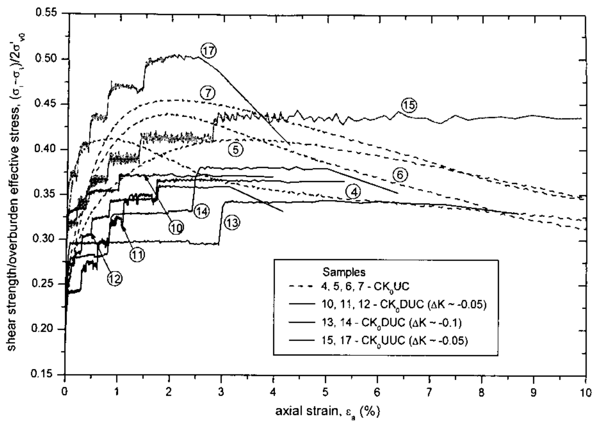

Fig. 5. Relationship between deviator stress (q) and axial strain (ε_a) of CK$_0$UC, CK$_0$DUC and CK$_0$UUC tests

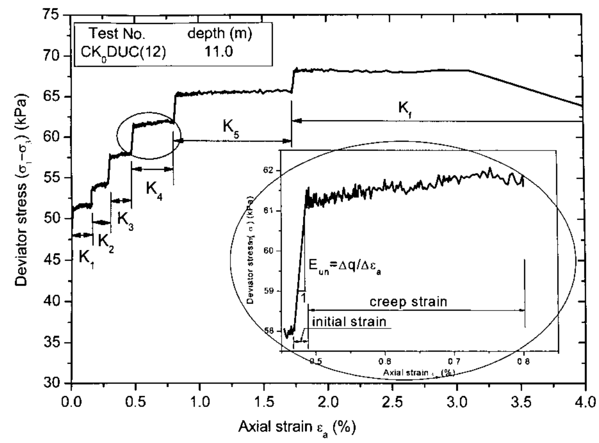

Fig. 6. Definition of Unloading Young's modulus E_{un}

Tanaka, H. et al. (2001).

In Figure 5, the ratio $[(\sigma_1-\sigma_3)/2]/\sigma'_{vo}$ of CK$_0$DUC tests of the samples below 6 m deep was less than 0.40 (except the sample of CK$_0$UUC test) and smaller than that ratio of CK$_0$UC tests. It could be explained based on primary concept of Hvorslev that the shear strength was composed of an effective friction increasing linearly with the effective stress and an effective cohesion. The cohesion component was mobilized with a small strain and would cause a gradual transfer of shear stresses to the more stable frictional contact points (Schmertmann and Osterberg, 1961). In the case of CK$_0$DUC test, the load was applied discontinuously by keeping the same state of effective stresses for 24 or 48 hours. Therefore, the cohesion component was not mobilized completely while the frictional strength was quickly mobilized by drained condition. As a result, the shear strength of clay of CK$_0$DUC tests was only equal to the residual strength of CK$_0$UC tests.

Many researchers studied the values of the ratio E_u/s_u on soft Bangkok clay. Their main purpose was to reduce the input parameters of elasto-perfectly plastic soil model for applying finite element analysis on the retaining wall structure. Some values of this ratio were predicted by the back analysis of the lateral displacement of the wall. They found that the ratio varied in the range of 200~500 (Bowels, 1988); 280~350 for soft clay and 1200~1600 for stiff clay (Hock, 1997); 500 and 2000 for soft Bangkok clay and stiff clay, respectively (W. Teparaksa et al., 1999). Actually, the ratio Eu/su was a function of many variables, e.g., the strain level (Mair, 1993), plasticity index and OCR (Duncan and Buchigani, 1976). As shown in Figure 5, the undrained shear strength absolutely depended on the strain value at which the ratio of shear strength and overburden effective stress $[(\sigma_1-\sigma_3)/2]/\sigma'_{vo}$ reached its peak.

Based on the relationship between deviator stress ($q = \sigma_1-\sigma_3$) and axial strain (ε_a) of CK$_0$UC tests, the ratio E_u/s_u was calculated with the undrained shear strength s_u at peak and the undrained Young's modulus with less than 0.01% axial strain $E_{u(0.01\%)}$. As shown in Figure 3, the E_u/s_u ratio was from 1100 to 1300 for weathered clay layer upper 4 m depth and from 600 to 800 for normal soft soil layer from 4 m to around 13 m depth. In addition, the undrained shear strength of CK$_0$UC tests was approximately close to the values of field-vane-shear tests $s_{u(FVS)}$; therefore, the E_u values at a small strain ($\varepsilon_a \leq$ 0.01%) could be estimated from $s_{u(FVS)}$ instead of undrained shear strength of unconfined compression test (UC). As a result, in the soft clay layer, the E_u/s_u ratio measured by CK$_0$UC tests was larger than that ratio determined by back finite element analysis of lateral displacement of the wall.

In CK$_0$DUC and CK$_0$UUC tests, the strain of each K-value step could be divided into two parts, initial and creep strains as shown in Figure 6. The initial strain happened immediately after applying the reduction of cell pressure value. At this moment, the pore water excess

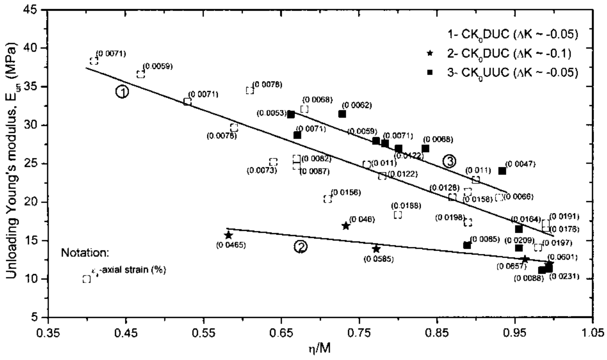

Fig. 7. Relationship between Unloading Young's modulus E_{un} and ratio η/M

was negative and the axial strain increased rapidly with an increase of deviator stress. As shown in the ellipse of Figure 6, the slope of the straight line which was the relationship between increment of deviator stress Δq and initial axial strain $\Delta\varepsilon_a$ was called unloading Young's modulus E_{un}.

In the unloading compression triaxial tests (CK_0DUC and CK_0UUC), the decrement step of horizontal pressure was controlled by the stress ratio ($K = \sigma'_h/\sigma'_v$) or the slope of stress path ($\eta = q/p'$) in p$'$-q plane. To obtain the desired stress ratio K, the cell pressure was controlled to unload with the stress rate of -1.0 kPa/min while the axial effective stress was controlled automatically to maintain as constant. In fact, the axial strain rate in CK_0DUC and CK_0UUC tests was not controlled and was larger than that value 0.1%/min of CK_0UC tests. Consequently, the unloading Young's modulus E_{un} of the first unloading step of CK_0DUC and CK_0UUC tests was greater than the Young's modulus E_u of CK_0UC tests because of the difference of axial strain.

The relationship between unloading Young's modulus E_{un} in CK_0DUC and CK_0DUC tests and the stress state was established based on the stress ratio ($\eta = q/p'$) and the slope of Critical State Line ($M = q_f/p'_f$) in p$'$-q plane. As shown in the lower right corner of Figure 8, the slope of the line, which was the relationship between deviator stress and mean effective stress, was called η ($\eta = q/p'$) at each decrement step of horizontal stress (K value) and M ($M = q_f/p'_f$) at the critical state. In Figure 7, the unloading Young's moduli E_{un}, which were calculated with the increment of axial strain $\Delta\varepsilon_a$ less than 0.02% (Figure 6), decreased with the ratio η/M. In other words, the Young's modulus of soil behind the diaphragm wall decreased during excavation process.

In Figure 7, the unloading Young's moduli were performed and shown signified by square (ΔK=-0.05) and solid star (ΔK=-0.1) symbols for CK_0DUC tests and solid square symbols for CK_0UUC tests. Lines 1 and 2 showed the relationship between the unloading Young's modulus E_{un} and the ratio η/M of two different values of the stress ratio decrement ΔK=-0.05 and ΔK=-0.1, respectively. On comparing line 1 and line 2, when the absolute value of the stress ratio decrement ΔK increased from 0.05 to 0.1, the unloading Young's modulus decreased and the initial axial strain (as shown in Figure 6) increased. Moreover, when the soil specimens were still strong enough ($\eta/M<0.85$), the E_{un} values of CK_0UUC tests were larger than those values of CK_0DUC tests as shown in lines 2 and 3. Thus the unloading Young's modulus depended on the amplitude of applied horizontal stress and the drainage condition of soil specimen. Furthermore, when the ratio η/M increased or the stress state of soil specimen approached the critical state, the unloading Young's modulus decreased and reached a lower bound around 12 MPa.

3.2 Slope of Critical State Line

Based on the data shown in Table 2, the slope of Critical State Line (M) of CK_0UC tests had two different values. The soil samples at upper 5.0 m deep were overconsolidated clay because of weathering effects, and the M values were around 2.0. Meanwhile, the soft soil sample at lower 5.0 m deep was lightly overconsolidated clay and the M values were equal to 1.50 ($\phi' = 37^0$) as shown in Figure 8. Compared with the M value 1.05 ($\phi' = 26^0$) obtained from series of isotropically consolidated undrained compression triaxial test (CIUC) of undisturbed specimens of soft Bangkok clay (Balasubramaniam, A. S. and Chaudry A. R., 1978) the M value around 1.5 of CK_0UC tests of this study was larger due to the difference of test procedures. However, when comparing with CK_0UC tests carried out by Tanaka H., et al. (2001) on

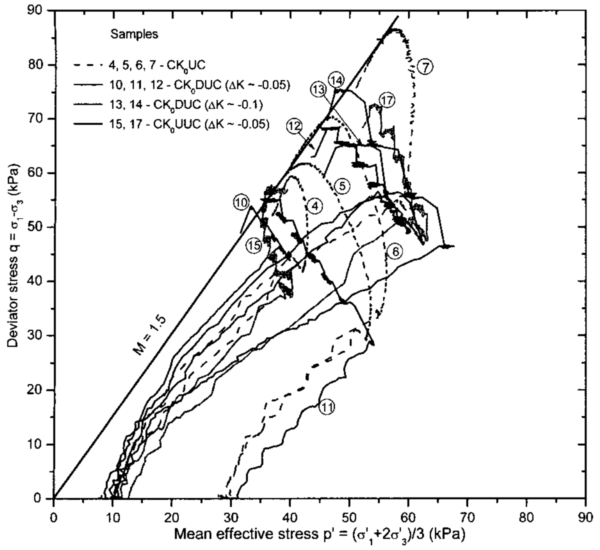

Fig. 8. Slope of the Critical State Line

Bangkok clay, the slope of the critical line was the same (M=1.5 or $\phi' = 37^0$). Furthermore, the CK_0UC triaxial test data on Bangkok Clay for Nong Ngoo Hao and Sutthisan sites reported by Shibuya et al. (1999) showed the internal friction angles (ϕ') to be 38^0 and 34^0, respectively.

From the results of CK_0UC tests in Table 2 the friction angles at peak and residual of stress ϕ'_p and ϕ'_r were larger than those values of CIUC tests. That could be explained by the differences of the orientation of principle stresses and the orientation and/or integration of the particles inside the soil specimen during isotropic and anisotropic consolidation process of CIUC and CK_0UC tests. In other words, if the isotropic consolidation pressure in CIUC test was set to be equal to or larger than in situ overburden stress intending the specimen to be normally consolidated state, then the change of micro-structure of the clay specimen (which was made during deposition and grown by subsequent ageing) occurred and the shear resistance decreased, which led to obtaining low ϕ' value comparing with CK_0UC test. Because the mean effective consolidation stress ($p' = (\sigma'_v + 2K_0 \times \sigma'_v)/3$) of CIUC test was larger than that value of CK_0UC test for the same vertical consolidation stress. The K_0 value was usually smaller than unity for the normally consolidated state. As a result, the ϕ' value of CIUC and CK_0UC tests was influenced by the magnitude of consolidation stress and consolidation stress system (isotropy or anisotropy) but not influenced by the shearing conditions.

Figure 8 showed the stress path of three series of CK_0UC, CK_0DUC and CK_0UUC tests. It should be noted that the 13 and 14 CK_0DUC tests were completed with the stress ratio decrement (ΔK) equal to -0.01, which was twice larger than that value of the 10, 11 and 12 CK_0DUC tests. However, the slope of Critical Sate Line (M) of those CK_0DUC tests was almost the same as that of CK_0UC and CK_0UUC tests. In other words, the M value of three kinds of triaxial test were approximately equal to 1.5 and did not depend on the amplitude of applied periodic load and the drainage condition.

3.3 Creep Deformation

Figures 9 (a) and 10 (a) showed the data of the axial and radial strains versus time obtained from CK_0DUC and CK_0UUC tests, respectively. The data of each K value stage were recorded for 24 hours except for the last stage (the rupture). The strains curves were fitted in by the logarithmic and exponential functions of time. The strain rate curves shown in Figures 9 (b) and 10 (b) were the derivative of strain functions. These curves immediately reached the large value after unloading horizontal pressure then they reduced virtually linear versus time. In other words, these strain rates were not constant during 24 hours of maintaining applied loading. The axial and radial strain rates of both CK_0DUC and CK_0UUC tests increased with deviator stress and decreased with time.

The strain rates of axial and lateral strain of five CK_0DUC tests (No. 8 to 12), shown in Figure 9, could be approximated by the linear logarithmic equations

$$\dot{\varepsilon}_a = a_a + b_a \log t \text{ - axial strain rate} \tag{1}$$

and $$\dot{\varepsilon}_r = a_r + b_r \log t \text{ - lateral strain rate.} \tag{2}$$

The coefficients a_a, b_a and a_r, b_r shown in Figures 12 and 13 related a linear line to the ratio $\eta/(M-\eta)$. In Figure 11, the strain rate of each η value of stress state was shown by one curve line. At the same value of time, the closer M value got η value, the larger absolute value of strain rate became. Hence, the strain rates increased when the

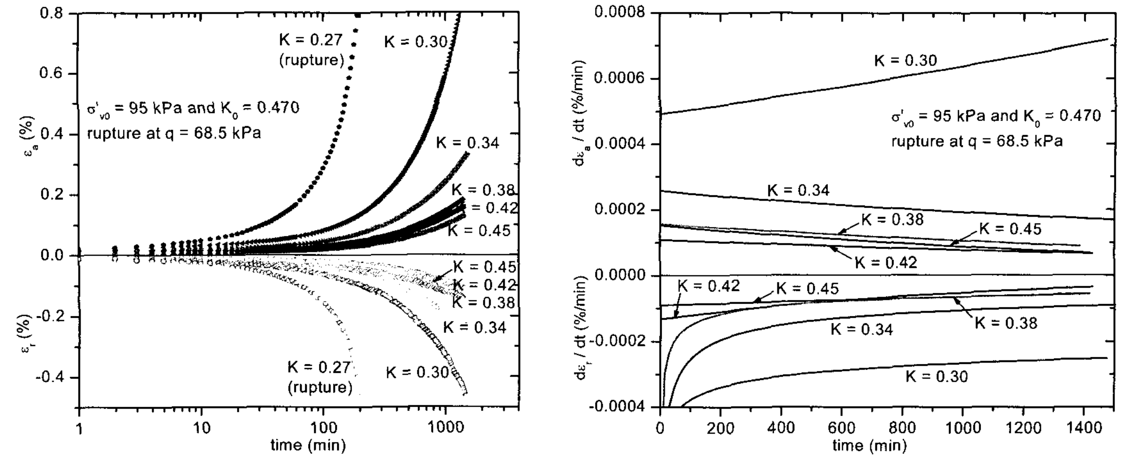

(a) (b)

Fig. 9. Strain and strain rate of soil sample at depth 11.0 m under CK0DUC test

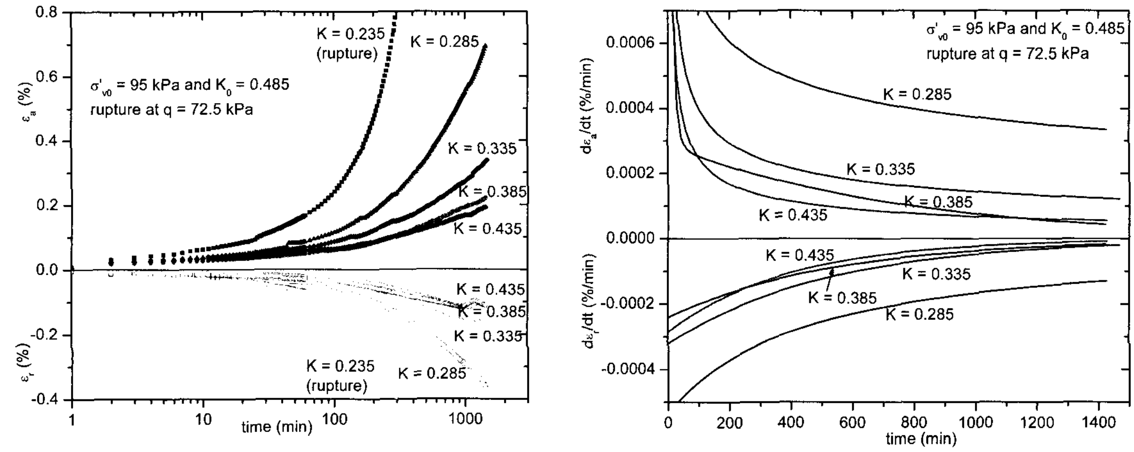

(a) (b)

Fig. 10. Strain and strain rate of soil sample at depth 11.0 m under CK0UUC test

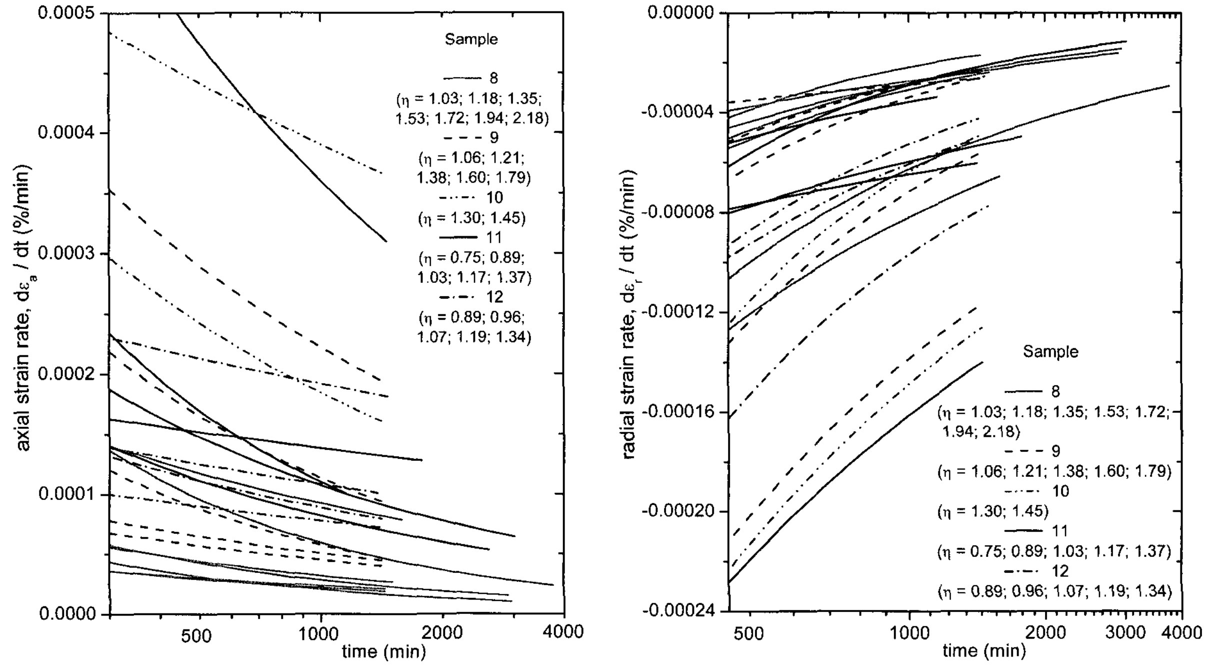

Fig. 11. Strain rate of soil sample under CK0DUC test

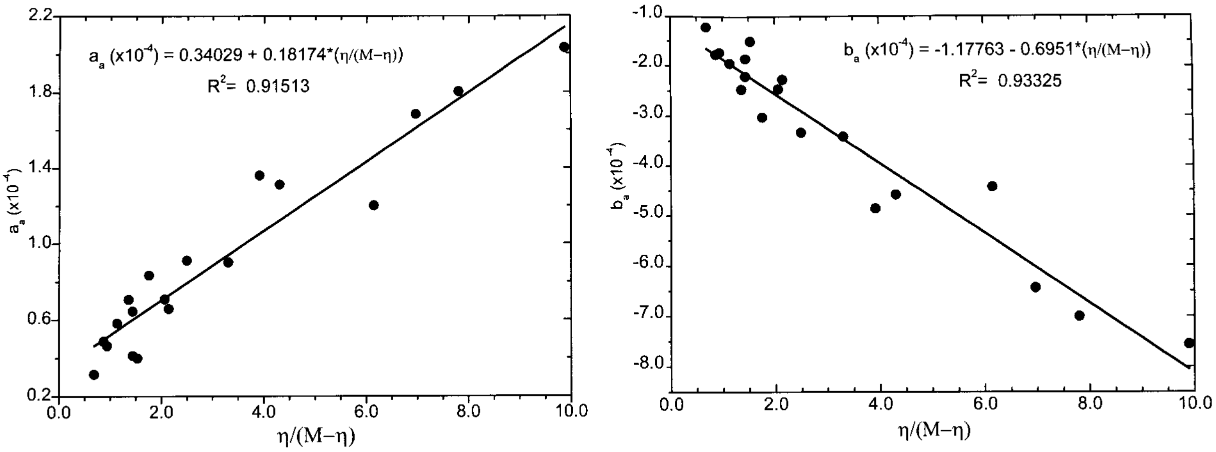

Fig. 12. Coefficient a_a and b_a of axial strain rate $\dot{\varepsilon}_a$

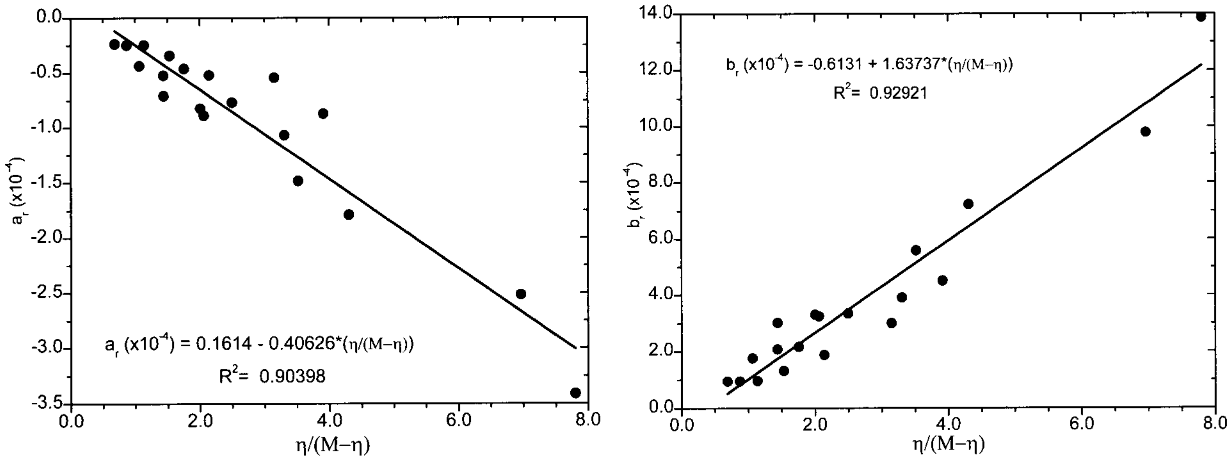

Fig. 13. Coefficient a_r and b_r of radial strain rate $\dot{\varepsilon}_r$

stress state approached the value of stresses at failure.

The coefficient of deformation with time (C_α) of clay soil was usually determined from vertical strain of oedometer test or the volumetric strain of the triaxial consolidation test. According to Tavenas F. et al. (1978), the expression of the relationship of C_α and strain rate was shown in Equation [3].

$$\dot{\varepsilon} = C_\alpha / t(1 + e_0) \text{ or } C_\alpha = \dot{\varepsilon} \times t \times (1 + e_0) \qquad (3)$$

while $\dot{\varepsilon}$ was axial strain rate of oedometer test or volume strain rate of triaxial test.

In the unloading compression triaxial test (CK_0DUC and CK_0UUC), both axial and radial strain rates were considered. From Equation [3], the coefficient of the deformation of both axial ($C_{\alpha a}$) and radial ($C_{\alpha r}$) directions could be calculated by substituting by $\dot{\varepsilon}_a$ and $\dot{\varepsilon}_r$.

$C_{\alpha a} = \dot{\varepsilon}_a \times t \times (1 + e_0)$ - coefficient of axial deformation (4)

and $C_{\alpha a} = \dot{\varepsilon}_r \times t \times (1 + e_0)$- coefficient of radial deformation (5)

Therefore, the coefficient of deformation as well as strain rate depended on the deviator stress level, time and the direction of deformation.

4. Conclusions

To determine the soil behavior at the elapse time of excavation behind the diaphragm wall of the Bank of Thailand project in Bangkok by means of top down construction, a series of triaxial testes (CK_0UC, CK_0DUC, and CK_0UUC) were performed. Based on the field vane-shear test and a series of triaxial tests, the following conclusions can be obtained.

(1) To predict the initial lateral displacement of the DW by using elasto-perfectly plastic model, the undrained Young's modulus of soil could be determined based on the ratio $s_u/E_{u(0.01\%)}$ with undrained shear strength at peak of CK_0UC test or field vane-shear test. From the results of CK_0UC test of the Bangkok clay at BOT project, the ratio $s_u/E_{u(0.01\%)}$ is from 1100 to 1300 for weathered clay layer upper 4 m deep and 600 to 800 for soft soil layer deeper than 4 m. The residual shear strength of clay should be taken from the CK_0UC test to secure the stability of DW in the case that the excavation takes a long time to complete. The ratio (s_u/σ'_{v0}) of undrained shear strength of FVS test as well as CK_0UC tests and overburden effective stress is around 0.45 at the depth from 5m to 13m.

(2) The unloading Young's modulus (E_{un}) depends on the amplitude of applied horizontal stress and the drainage condition of soil specimen. As the stress state of soil specimen approaches the critical state or the ratio h/M increases, the unloading Young's modulus decreased and reached a lower bound around 12 MPa for soft Bangkok clay.

(3) For the soft Bangkok clay below 5.0 m deep without the effect of weathering consolidation, the Slope of Critical State Line (M) is equal to 1.5 for three kinds of CK_0UC, CK_0DUC and CK_0UUC tests. In other words, the M value does not depend on the amplitude of applied periodic load and the drainage condition.

(4) According to the results obtained from CK_0DUC and CK_0UUC tests, the coefficient of deformation with time (C_α) as well as strain rate depends not only on the deviator stress level, elapsed time and drainage condition but also on the direction of deformation. The coefficient of horizontal deformation ($C_{\alpha r}$) could be applied for FEM analysis to predict the lateral displacement of the DW versus time.

Acknowledgements

The triaxial tests were carried out at Soil Mechanics Laboratory of Hokkaido University and Hakodate National College of Technology. Thanks to Japan International Cooperation Agency (JICA) and ASEAN University Network / Southeast Asia Engineering Education Development (AUN/SEED-Net) for financial support of this research and the collaborative research between Chulalongkorn University of Thailand and Hokkaido University of Japan.

NOTATION

a_a, b_a	coefficients of the line of axial strain rate
a_r, b_r	coefficients of the line of radial strain rate
B-value	pore water parameter, $\Delta u/\Delta \sigma$
CK_0DUC	K_0 consolidated drained unloading compression triaxial test with periodic decrement of horizontal pressure
CK_0UUC	K_0 consolidated undrained unloading compression triaxial test with periodic decrement of horizontal pressure
CK_0UC	K_0 consolidated undrained compression triaxial test
C_α	coefficient of deformation
$C_{\alpha a}$	coefficient of axial deformation
$C_{\alpha r}$	coefficient of radial deformation
E_u	undrained Young's modulus
$E_{u\,(0.01\%)}$	undrained Young's modulus at 0.01% of axial strain
E_{un}	unloading Young's modulus
FVS	field-vane-shear test
K	lateral stress ratio, σ'_h / σ'_v
K_0	coefficient of earth pressure at rest, σ'_{h0} / σ'_{v0}
K_f	ratio of effective stress at failure, σ'_{hf} / σ'_{vf}
LL	liquid limit
M	slope of Critical State Line, q_f / p'_f
OCR	overconsolidation ratio
PL	plastic limit
p'	mean effective stress, $(\sigma'_1 + 2\sigma'_3)/3$
q	deviator stress, $(\sigma_1-\sigma_3)/2$
q_{max}	deviator stress at peak
s_u	undrained shear strength
$s_{u(FVS)}$	undrained shear strength of field-vane-shear test

t	time
UC	unconfined compression test
w	water content
γ_t	natural unit weight
ΔK	stress ratio decrement
ε_a	axial strain
ε_r	radial strain
$\dot{\varepsilon}$	strain rate
$\dot{\varepsilon}_a$	axial strain rate
$\dot{\varepsilon}_r$	radial strain rate
η	stress ratio, q/p'
ν	Poisson's ratio
σ_1	axial stress
σ_3	radial stress
σ'_1	axial effective stress
σ'_3	radial effective stress
σ'_{v0}	overburden effective stress
ϕ'	friction angle
ϕ'_p	friction angle at peak of stress
ϕ'_r	friction angle at residual stress

References

1. Balasubramaniam, A. S. and Chaudhry, A. R. (1978), "Deformation and Strength Characteristics of Soft Bangkok Clay", *Journal of the Geotechnical Engineering Division, ASCE*, 104 (9), 1153-1167.
2. Bjerrum, L. (1973), "Problems of soil mechanics and construction on soft clays and structurally unstable soils", State-of-the-art report, Session IV, *Proc. 8th Int. Conf. Soil. Mech. and Found. Eng.*, Moscow, 3, 111-159.
3. Malcolm Puller, CEng, DIC, FICE, FIStrucE (2003), *Deep Excavation a practical manual*, Thomas Telford Publishing, Thomas Telford Services Ltd., 1 Heron Quay, London E14 4JD, 571p.
4. Mitchell, J. K. and Soga, K. (2005), *Fundamentals of Soil Behavior*, Chapter 12, John Wiley & Sons.
5. Le, T. N., Teparaksa, W., Mitachi, T., Kawaguchi, T. (2006), "Observation of the Behavior of Soil Element behind Deep Diaphragm Wall by Triaxial Tests on Bangkok Clay", *Proceeding of 19th KKCNN Symposium on Civil Engineering*, Kyoto, Japan, 57-60.
6. Ou, C. Y., Liao, J. T., and Lin, H. D. (1998), "Performance of Diaphragm wall constructed using Top-down method", *Journal of Geotechnical and Geoenvironmental Engineering*, ASCE, 124 (9), 798-808.
7. Shibuya, S., Mitachi, T., Tanaka, H., Kawaguchi, T., and Lee, I. M. (1999) "Measurement and application of quasi-elastic properties in geotechnical site characterization", *Proceeding of 11th Asian Regional Conference on SMGE*, Seoul, Korea, 85-156.
8. "Standards of Japanese Geotechnical Society for Laboratory Shear Test (English Version)" (1999), The Japanese Geotechnical Society, 110p.
9. Tanaka, H., Locat, H., Shibuya, S., Soon, T. T. (2001), "Characterization of Singapore, Bangkok, and Ariake clays", *Canadian Geotechnical Journal*, 38, 378-400.
10. Tavenas, F., Leroueil, S., LaRochelle, P., and Roy, M. (1978), "Creep behaviour of an undisturbed lightly overconsolidated clay", *Canadian Geotechnical Journal*, 15, 402-423.
11. Teparaksa, W. (1999), "Analysis of lateral wall movement for deep braced excavation of Bangkok subsoils", *Proceedings of Civil and Environmental Engineering Conference New Frontiers & Challenges*, 8-12 November 1999, Bangkok, Thailand, 2 (I), 67-76.

(received on Mar. 27, 2007, accepted on Jul. 23, 2007)